Monatsh Chem 139, 739–745 (2008)
DOI 10.1007/s00706-007-0835-7
Printed in The Netherlands

Monatshefte für Chemie
Chemical Monthly

Polyhalite and its analogous triple salts

Georgia Wollmann, Daniela Freyer, Wolfgang Voigt

Institut für Anorganische Chemie, TU Bergakademie Freiberg, Freiberg, Germany

Received 1 August 2007; Accepted 23 October 2007; Published online 9 June 2008
© Springer-Verlag 2008

Abstract Polyhalite ($K_2SO_4 \cdot MgSO_4 \cdot 2CaSO_4 \cdot 2H_2O$) and analogue triple salts, where Mg^{2+} is substituted by Mn^{2+}, Fe^{2+}, Co^{2+}, Ni^{2+}, Cu^{2+} and Zn^{2+}, have been synthesized. The salts were characterized by thermal analysis, *Raman* spectroscopy and X-ray powder diffraction.

Diffraction patterns and *Raman* spectra resemble those of natural polyhalite, except $K_2SO_4 \cdot CuSO_4 \cdot 2CaSO_4 \cdot 2H_2O$. The latter corresponds to the mineral leightonite, which is structurally different.

For polyhalite analogues the cell parameters of the triclinic unit cell have been determined from the powder diffraction patterns. The length of the unit cell vectors varies regularly with the ionic radius of the substituted ion M^{2+} and is explained by changes in the extension of the coordination octahedron of M^{2+}. Thereby increasing distances of the coordinated water molecules at M^{2+} parallel with decreasing dehydration temperatures of the corresponding polyhalite.

Keywords Polyhalite; Leightonite; *Raman* spectroscopy.

Introduction

Polyhalite, $K_2MgCa_2(SO_4)_4 \cdot 2H_2O$, belongs to the most abundant minerals in rock salt formations. Several publications regarding the crystallization field of polyhalite appeared [1–16] during the past century. Studies on the thermal behaviour of polyhalite were required in respect to the storage of nuclear waste in rock salt deposits [17, 18]. Although polyhalite is a relatively common mineral, the crystal structure was solved not until 1970 [19, 20]. This is due to the distinctive twinning and small size of the salt crystals.

The existence of a series of polyhalite analogue triple salts $A_2MCa_2(SO_4)_4 \cdot 2H_2O$ with $A = K^+$, $NH_4{}^+$ and $M = Mn^{2+}$, Fe^{2+}, Co^{2+}, Ni^{2+}, Cu^{2+}, Zn^{2+}, Cd^{2+} was already reported by *D'Ans* in 1908 [21]. However, he did not describe details of preparation, only the chemical composition was stated.

In 1938 *Palache* discovered a new pale blue mineral in Chile, which later was named leightonite [22]. According to chemical analytical examinations the mineral represents a copper analogue of polyhalite.

Up to now, there are no investigations on the characterization of the polyhalite analogue triple salts reported by *D'Ans*, except of the crystal structure of the copper analogue – leightonite. From optical examinations *Palache* stated a triclinic-pseudorhombic unit cell as for polyhalite. *Van Loan* found an orthorhombic unit cell according to the X-ray powder pattern [23] and *Menchetti et al.* determined a monoclinic unit cell on the basis of a single crystal analysis at a natural leightonite twin [24].

The aim of this work is to find convenient conditions for the preparation of the polyhalite analogue triple salts and to characterize the synthesized salts by thermal analysis, *Raman* spectroscopy and X-ray powder diffraction.

Correspondence: Daniela Freyer, Institut für Anorganische Chemie, TU Bergakademie Freiberg, 09599 Freiberg, Germany. E-mail: daniela.freyer@chemie.tu-freiberg.de

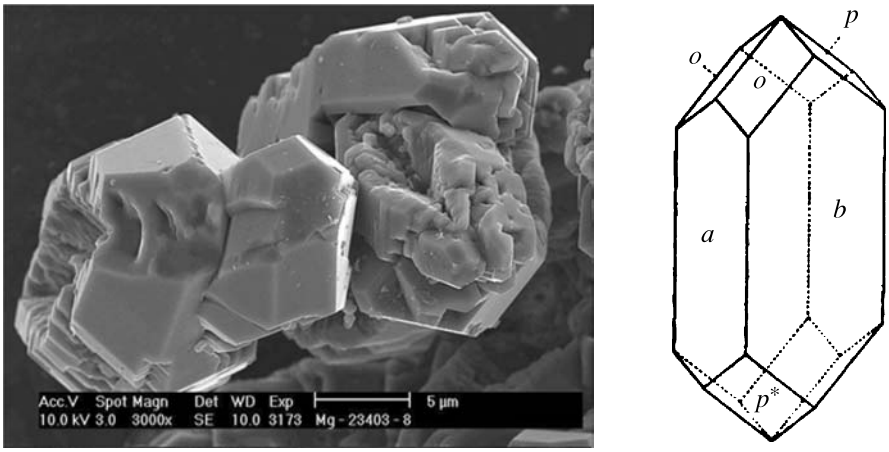

Fig. 1 SEM of an obtained polyhalite in comparison with a polyhalite crystal sketch by *Görgey* [25]

Results and discussion

Morphological characteristics

The obtained crystals of polyhalite and its analogues were too small (max. 50 μm) for a proper inspection using optical microscopy. For this reason scanning electron micrographs (SEM) were taken.

Figure 1 shows polyhalite crystals at a magnification of 3000. As can be seen the crystals are quite small and crystal faces are not well developed. Nevertheless the shape resembles closely *Görgey*'s sketch of a natural polyhalite crystal [25]. The main difference that can be noticed concerns the side faces of the polyhedron. *Görgey*'s polyhalite has only 4 side faces, while the obtained crystals present 6.

The synthesized leightonite crystals shown in Fig. 2 can be described best as square bipyramids.

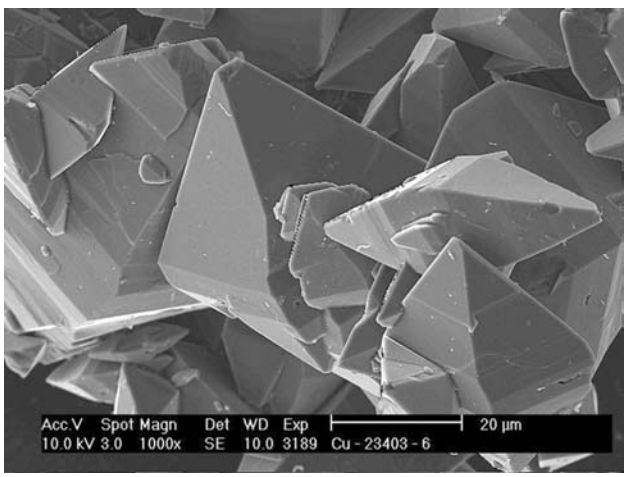

Fig. 2 SEM of an obtained leightonite

Table 1 Thermal dehydration characteristics of polyhalite and its analogues

Compound	Theoretical mass loss/%	Practical mass loss/%	t_{onset}/ °C	t_{peak}/ °C
Polyhalite	5.97	5.9	255	343
Mn-polyhalite	5.69	5.7	185	280
Fe-polyhalite	5.68	5.5	290	326
Co-polyhalite	5.65	5.5	243	347
Ni-polyhalite	5.65	5.5	273	393
Leightonite	5.61	5.7	311	372
Zn-polyhalite	5.59	5.6	240	330

A remarkable degree of intergrowth can be recognized. Compared with common polyhalite the crystal faces of leightonite are better developed.

Thermal analysis

In Table 1 the thermal dehydration data are collected. Comparison of columns 2 and 3 confirms the water content of the polyhalite formula within 0.1%. As can be seen in the thermal release diagrams (Fig. 3) ranges of different dehydration rates occur, which cannot be resolved into single steps. Depending on the substituted cation the dehydration temperature varies from 185 to 311°C at onset of the peak and from 280 to 393°C at the peak maxima. The latter temperatures θ_{peak} correlate with the radius of the M^{2+} ions $r_{M^{2+}}$ in an octahedral coordination (Fig. 4). The thermal effects after completed dehydration were not further investigated. They are caused by a variety of solid state reactions and transformations as earlier discussed in more detail [17].

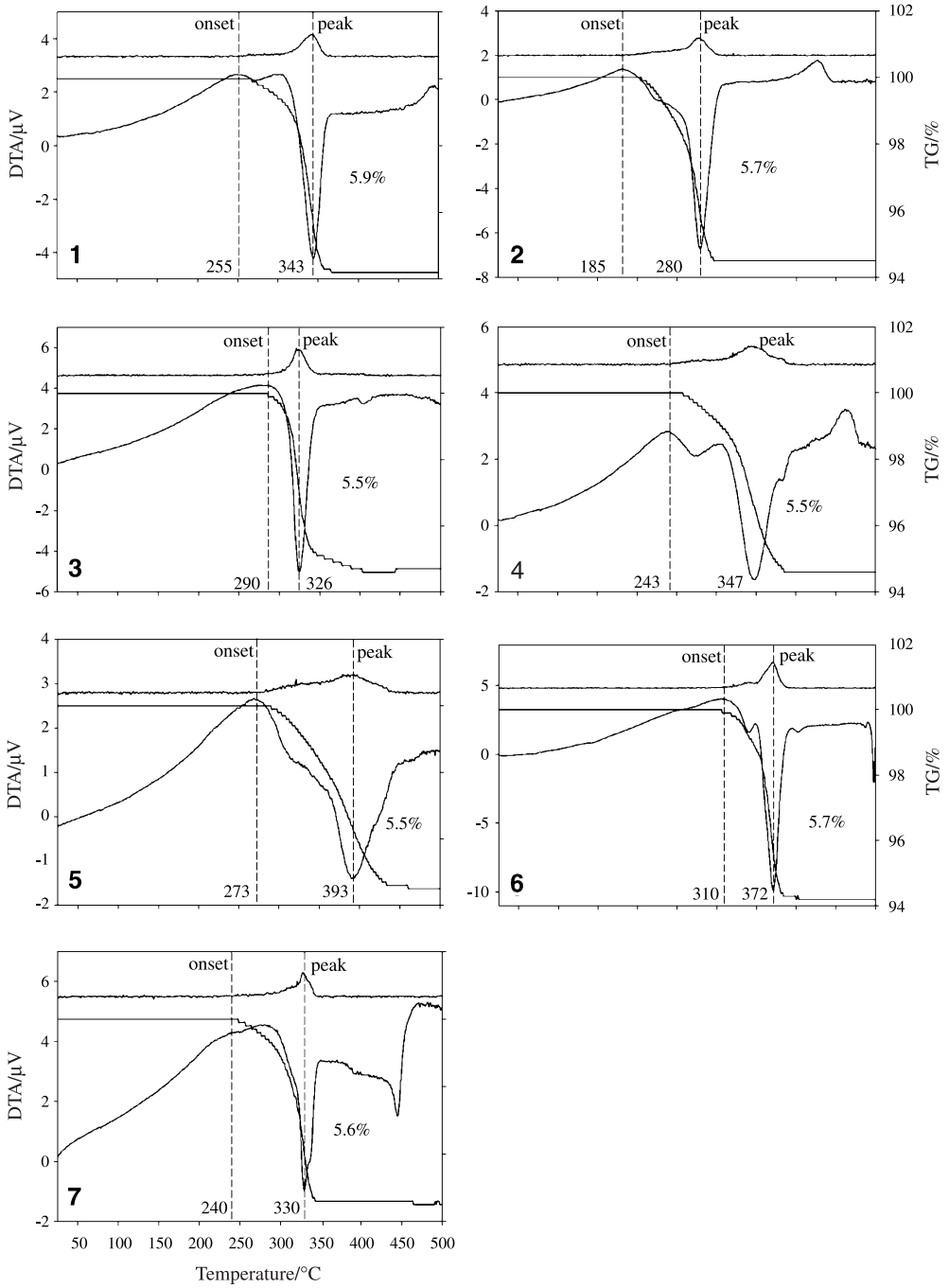

Fig. 3 Thermal analysis diagrams with TG, DTA, DTG (axis not shown); *1* polyhalite, *2* Mn-polyhalite, *3* Fe-polyhalite, *4* Co-polyhalite, *5* Ni-polyhalite, *6* leightonite, *7* Zn-polyhalite

Raman spectroscopy

The comparison of the *Raman* spectra of polyhalite and its analogues (Fig. 5) reveals similarity of all spectra except the spectrum of leightonite. Major differences can be noticed in the range of sulphate stretch vibrations at about 1000 cm^{-1}. In this region leightonite possesses only one broad *Raman* band, while in the other compounds this band is splitted into two. A regular shift of the symmetric stretching vibration of the sulphate ion occurs. (in cm^{-1} Mg: 991, 1017; Mn: 987, 1010; Fe: 983, 1009; Co: 982, 1010; Ni: 983, 1011; and Zn: 986, 1011).

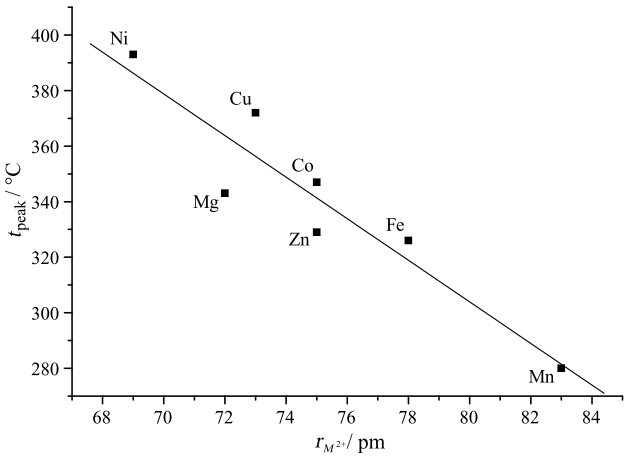

Fig. 4 Correlation of the temperature of dehydration and the ionic radius

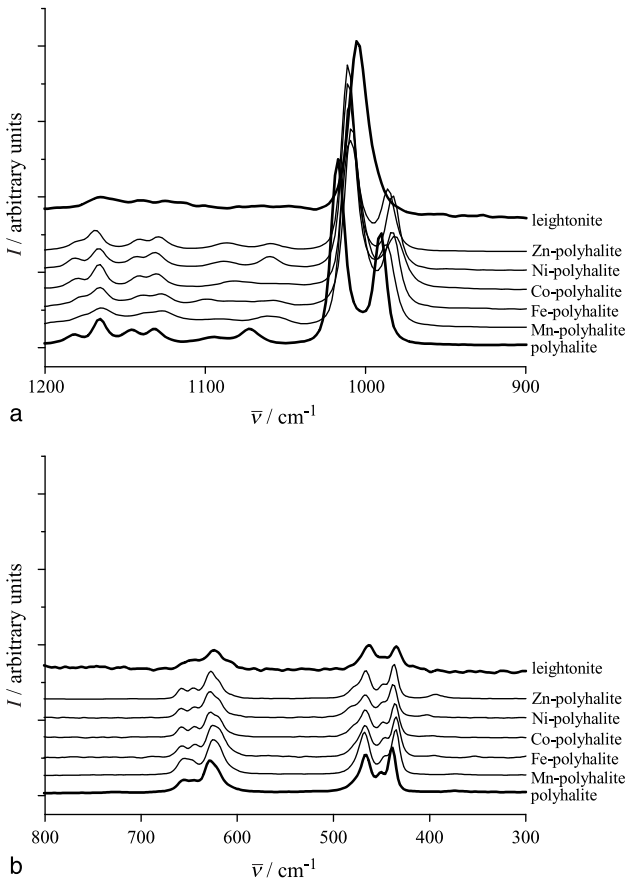

Fig. 5a,b *Raman* spectra of polyhalite and its analogue

X-Ray powder diffraction

The recorded powder pattern of synthesized polyhalite (Fig. 6) agrees with both patterns simulated from single crystal structure data [19, 20] using the program POWDERCELL [26] and thus confirms structural identity.

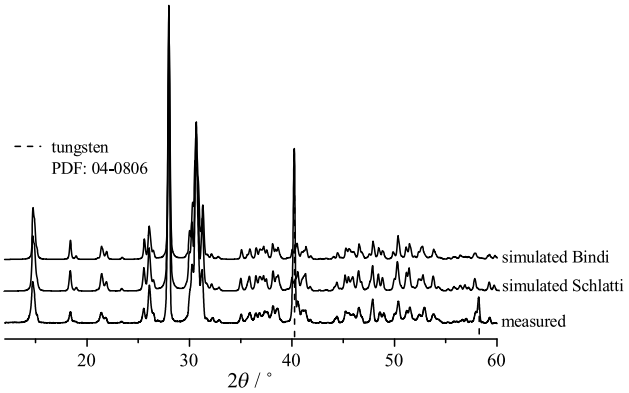

Fig. 6 Measured pattern of synthesized polyhalite and simulated X-ray powder diffraction of single crystal data by *Schlatti et al.* [19] and *Bindi* [20]

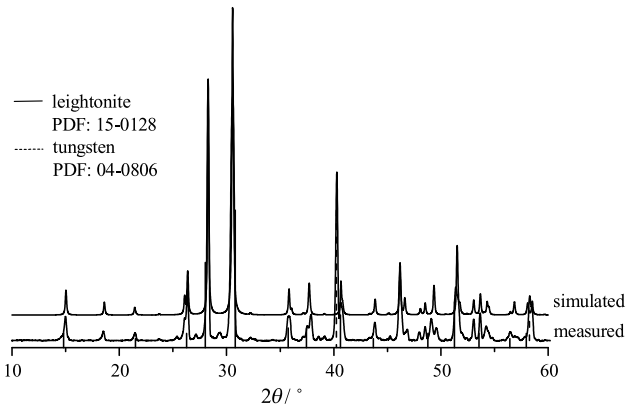

Fig. 7 X-ray powder diffraction pattern of synthesized leightonite, vertical lines: PDF 15-0128, simulated pattern from crystal structure data by *Menchett et al.* [24]

The X-ray powder pattern of leightonite (Fig. 7) have been compared with reflexes of the PDF-database (PDF 15-0128) measured by *van Loan* [23]. As can be seen, some peaks are slightly shifted and additional peaks occur in the recorded pattern.

With data of the single crystal analysis of natural leightonite [24] a powder pattern was simulated (Fig. 7). In general the simulated and the measured pattern look similar. The peaks of high intensities are the same in both patterns.

The powder patterns of the other polyhalite analogue compounds resemble that of polyhalite (Fig. 8). This indicates that all belong to the same crystal structure type except leightonite.

Essential differences in the peak pattern between leightonite and the other triple salts can be recognized in the ranges 25–34° and 35–60° (Fig. 8). Values of d-spacing of the most intensive reflexes of all triple salts are listed in Table 2.

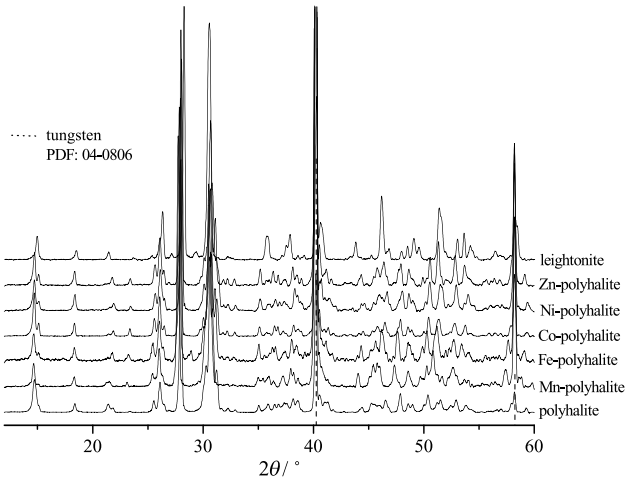

Fig. 8 Powder diffraction pattern of polyhalite and its analogue compounds

For the polyhalite analogues the powder diagrams were treated with the peak fitting program PROFILE [27] to determine peak positions for unresolved reflexes. Nine reflexes were applied for lattice parameter refinement calculations performed with the program CELREF [28]. As starting values the unit cell parameters of polyhalite published by *Schlatti et al.* had been used after transforming from the F-1 cell into a P-1 cell. The calculated lattice parameters are listed in Table 3 together with the ionic radius of M^{2+} ions taken from [29].

Variation of the unit cell axes and volume with ionic radius of M^{2+} is plotted in Fig. 9. Increasing the ionic radius of M^{2+} causes expansion of the cell in a and b direction and contraction in direction of c. Thereby the effect on the b-axis is approximately two times as large as on the a – axis. Increased length of the b axis indicates weakening of water coordination at the M^{2+} ion. The angles of the unit cell alter also systematically, but are not easily to discuss.

In Figure 10 the orientation of the coordination octahedron of the bivalent metal ion is shown in respect to cell axes. The metal ion is surrounded by four sulphate oxygens and two water oxygens. Location of the water molecules is almost along the b-axis, while the sulphate oxygens are almost in the a-c-plane. The increase of the length of the b-axis could be caused by enlarged M^{2+}-water distances, which means weaker coordination of water. The enhanced distance of the water molecules allows the sulphate oxygen to approach closer to the metal ion. This leads to the observed contraction of the c-axis. In the direction of the a-axis the effects are partly compensating each other. Macroscopically the weaker coordination of water is reflected in decreasing dehydration temperatures as listed in Table 2.

Table 2 Values of d-spacing of the most intensive X-ray diffraction reflexes of all triple salts

d/Å						
Polyhalite	Mn-polyhalite	Fe-polyhalite	Co-polyhalite	Ni-polyhalite	Zn-polyhalite	Leightonite
6.010	6.037	6.019	6.018	5.994	6.006	5.933
3.413	3.421	3.412	3.414	3.402	3.409	3.388
3.186	3.212	3.196	3.188	3.172	3.184	3.158
2.973	2.927	2.967	2.921	2.963	2.967	2.927
2.951	2.897	2.912	2.901	2.895	2.911	2.224
2.913	2.225	2.871	2.859	2.861	2.872	1.967
2.861	1.795	1.782	2.224	2.213	2.224	1.779
2.223				1.803	1.779	
1.900						

Table 3 Lattice parameters of polyhalite and its analogues

Compound	$r_{M^{2+}}$/pm	a/Å	b/Å	c/Å	α/°	β/°	γ/°	V/Å^3
Polyhalite	72	6.98	6.97	8.94	101.2	104.1	113.9	364.28
Mn-polyhalite	83	7.13	7.28	8.82	102.8	102.7	115.4	376.48
Fe-polyhalite	78	7.08	7.14	8.88	102.1	102.5	114.9	373.62
Co-polyhalite	75	7.04	7.01	8.90	101.3	104.1	114.2	366.03
Ni-polyhalite	69	6.96	6.97	8.97	101.1	104.5	113.9	363.05
Zn-polyhalite	75	6.98	6.99	8.93	101.3	104.1	114.0	364.15

The uncertainties are: for a, b, $c \pm 0.02$ Å, for α, β, γ $\pm 0.2°$, for $V \pm 1.1$ Å^3

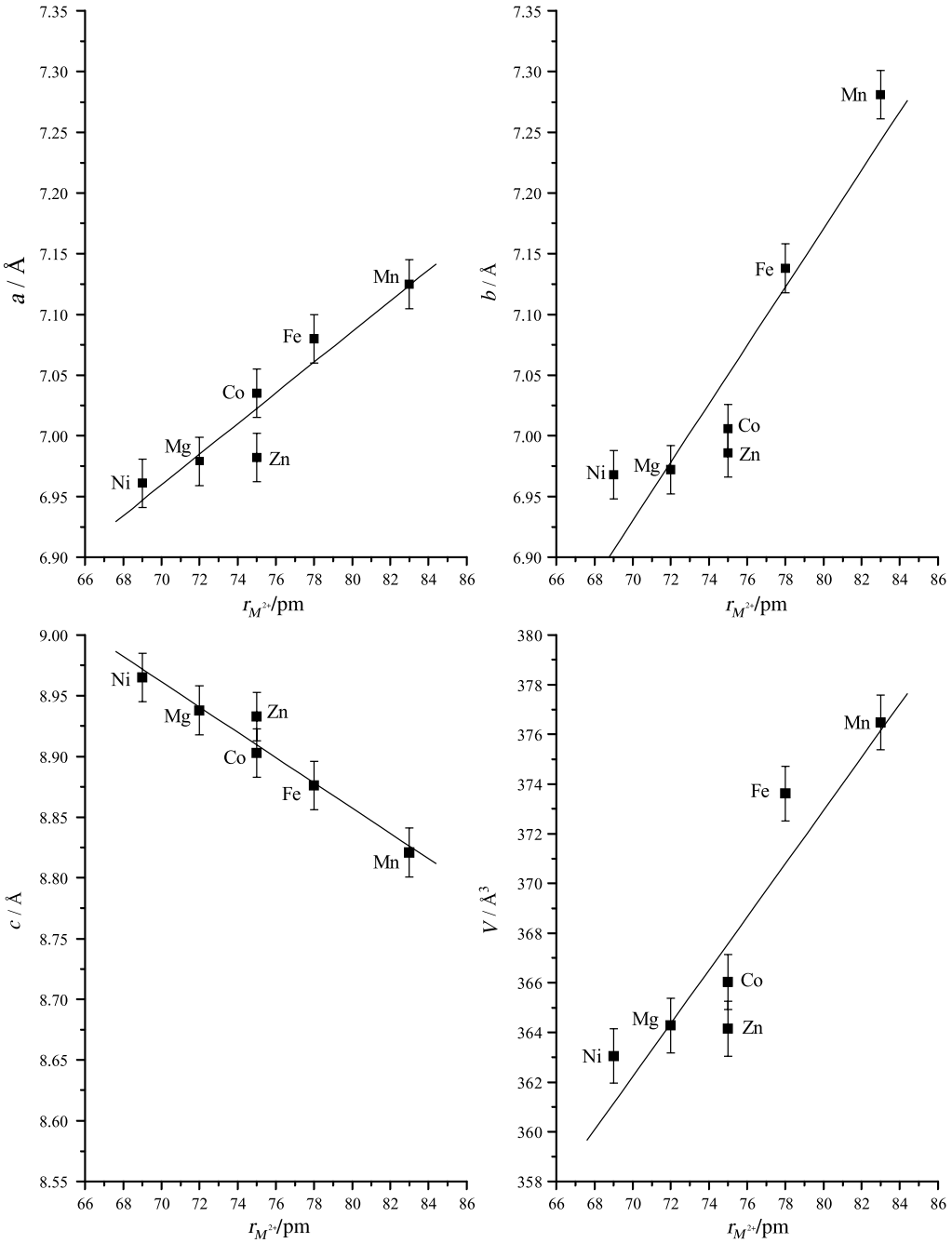

Fig. 9 Correlation of the unit cell parameters with the ionic radius

Experimental

Preparation of the triple salts $K_2MCa_2(SO_4)_4 \cdot 2H_2O$ ($M =$ Mn^{2+}, Fe^{2+}, Co^{2+}, Ni^{2+}, Cu^{2+}, and Zn^{2+}) was carried out as follows.

In 150 cm^3 deionised water potassium sulphate (p.a. Reachim) and the appropriate metal sulphate (p.a. Merck, Fluka) were dissolved at the boiling point. The solution containing copper were handled at a *pH* around 4, to prevent the formation of basic copper sulphates. After 1.5 h the solid remaining was filtered off over a pre-heated fritted disk. Again, the solution was heated up to the boiling point and solid $CaSO_4 \cdot 2H_2O$ or $CaCl_2$ solution (1.8 mol/dm^3) was added. In Table 4 the compositions of the initial solutions are given. The reaction with gypsum required about 60 h, while with $CaCl_2$ solution the reaction was completed within 6 h. After the reaction time the products were separated over a pre-heated fritted disk and washed with 15 cm^3 85 and 96% ethanol each.

The Mg-polyhalite was prepared from solutions of the quinary system K^+, Mg^{2+}, Ca^{2+}/Cl^-, $SO_4{}^{2-}/H_2O$ as described in a paper of *Autenrieth* [1].

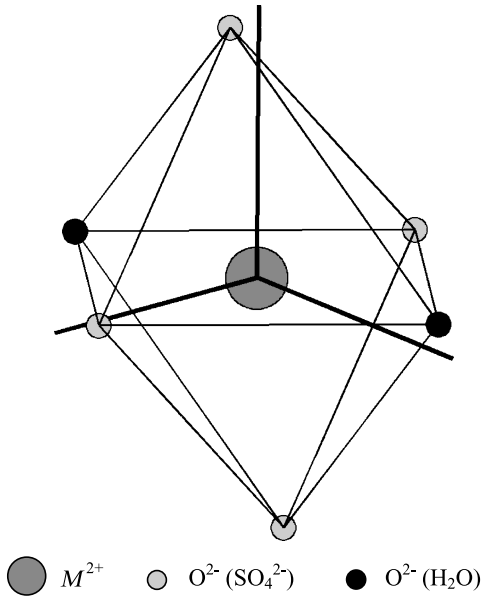

Fig. 10 Orientation of the M^{2+} coordination octahedron in respect to the axes of the triclinic unit cell

Table 4 Composition of the solutions for synthesis of the polyhalite analogue compounds

Compound	V_{H_2O}/ cm^3	m_{MSO_4}/ mol	$m_{K_2SO_4}$/ mol	$m_{CaSO_4 \cdot 2H_2O}$/ mol	$V_{CaCl_2\ sol}$/ cm^3
Mn-polyhalite	150	0.17	0.042	0.0081 –	– 9
Fe-polyhalite	150	0.12	0.040	0.0052 –	– 9
Co-polyhalite	150	0.12	0.040	0.0052 –	– 9
Ni-polyhalite	150	0.16	0.040	0.0052 –	– 9
Leightonite	150	0.062	0.022	0.0070 –	– 10
Zn-polyhalite	150	0.12	0.040	0.0052 –	– 9

All samples were characterized by thermal analysis, *Raman* spectroscopy and X-ray powder diffraction.

The thermal analysis was performed with a DTA/TG 22 (Seiko), with 10–20 mg of sample in a crucible of aluminium at a heating rate 5 K/min up to 500°C under nitrogen flow.

Raman spectra were recorded with a FT-spectrometer RFS 100/S (Bruker). The sample were filled into holders of aluminium and measured from 1200 to 350 cm^{-1} with a 1064 nm laser and a power of 75 mW at 200 cycles.

Powder X-ray diffraction patterns were obtained with a D5000 (Siemens) using CuKα radiation. All samples were mixed with tungsten as internal standard and measured in steps of 0.01° at a scan rate of 8 s.

The SEM pictures were taken with the electron microscope XL 30 (Philips) at a voltage of 10 kV at samples covered with carbon.

Acknowledgements

We thank the Projektträger Entsorgung at FZ Karlsruhe of the Federal Ministry for Education, Research and Technology (BMBF) Germany, for financial support.

References

1. Autenrieth H (1958) Kali Steinsalz 2:181
2. Autenrieth H, Braune G (1959) Kali Steinsalz 2:395
3. Bodaleva NV, Lepeshkov IN (1956) Zh Neorg Khim 1:995
4. Conley JE, Gabriel A, Partridge EP (1938) J Phys Chem 42:587
5. D'Ans J (1915) Kali 17:261
6. Dankiewicz J, Pawlowska-Kozinska D (1982) Z Anorg Allg Chem 488:223
7. Harvie CE, Eugster HP, Weare JH (1982) Geochim Cosmochim Ac 46:1603
8. Kropp E, Beate R, Grosch Ch, Kranz M, Holldorf H (1988) Freiberg Forschungsh A 764:42
9. Lepeshkov IN, Novikova LV (1958) Zh Neorg Khim 3:2395
10. Perova AP (1970) Zh Neorg Khim 15:1648
11. Perova AP (1970) Zh Neorg Khim 15:1927
12. Perova AP (1970) Zh Neorg Khim 15:2821
13. Perova AP (1973) Zh Neorg Khim 18:1970
14. Perova AP (1973) Zh Neorg Khim 18:2531
15. van't Hoff JH (1905) Z Anorg Chem 47:244
16. van't Hoff JH, D'Ans J (1906) Sitz-Ber Königl Preuss Akad Wiss, p 412
17. Fischer S, Voigt W, Köhnke K (1996) Cryst Res Technol 31:87
18. Jockwer NJ (1981) Kali und Steinsalz 8:126
19. Schlatti M, Sahl K, Zemann A, Zemann J (1970) Tschermaks Miner u Petrogr Mitt 14:75
20. Bindi L (2005) Acta Cryst E Structure Reports Online 61:i135
21. D'Ans J (1908) Ber dt Chem Gesellschaft 41:1777
22. Palache C (1938) Amer Min 23:34
23. van Loan PR (1962) Can Mineral 7:272
24. Menchetti S, Bindi L, Bonazzi P, Olmi F (2002) Amer Min 87:721
25. Görgey R (1914) Tschermaks Miner u Petrogr Mitt 33:48
26. Kraus W, Nolze G (2000) Powdercell Version 2.4, Federal Institute for Materials Research and Testing, Rudower Chaussee 5, 12489 Berlin, Germany
27. Jacob W, Smith K (1996) Profile Plus Version 1.06 DIFFRACplus package, Bruker AXS GmbH
28. Laugier J, Bochu B, celref V3 (2003) Laboratoire des Matériaux et du Génie Physique, Ecole Nationale Supérieure de Physique de Grenoble (INPG), Domaine Universitaire BP 46, 38402 Saint Martin d'Hères, France
29. Marcus Y (1997) Ion Properties, Marcel Dekker Inc., New York